

# Optimization of The Mechanical Drive on Set-up of Homemade Surface Plasmon Resonance

Muhammad Arifin, Febrilian Dwi Laksono, Supardianningsih, Kamsul Abraha

Department of Physics, Faculty of Mathematics and Natural Sciences, Universitas Gadjah Mada  
Sekip Utara, Bulaksumur, Yogyakarta 55281

Email: muhammad.arifin@ugm.ac.id

*Received 28 August 2017, Revised 27 September 2017, Accepted 2 October 2017*

**Abstract:** Mechanical optimization has been done on the surface plasmon resonance (SPR) homemade. At set-up, angle scanning comes a small resolution to detect changes in the thickness of the thin film or refractive index of the sample. The mechanical drive has a function to rotate the prism and detector. Torsional Spring-Loaded Gear Antibacklash is used to improve the accuracy of the mechanical drive. The stepper motor is used to rotate the mechanical drive automatically. The built system has successfully increased the resolution of the prism rotation angle by  $0.01^\circ$ . The test using the blank prism indicates the angle of Total Internal Reflection occurs at an incident angle of  $41.80^\circ$ . The SPR phenomenon was observed in a thin layer of gold deposited on the prism using a vacuum evaporator. The observed SPR angles on samples A, B, C, D, E, F, G, H and I were  $45.02^\circ$ ,  $45.05^\circ$ ,  $46.30^\circ$ ,  $44.48^\circ$ ,  $44.70^\circ$ ,  $45.49^\circ$ ,  $45.52^\circ$ ,  $45.66^\circ$ , and  $44.44^\circ$ , respectively. The SPR angle change shows the difference in the thickness of the gold thin film.

**Keyword:** optimization, mechanical drive, antibacklash, SPR angle

## 1. Introduction

The design of homemade surface plasmon resonance (SPR) set-up at the Department of Physics, Faculty of Mathematics and Natural Sciences Universitas Gadjah Mada was first built by Nasbey (2009) using a single wavelength. Improvements in the mechanical drive of the prism have been made by Arifin (2011) to produce angle variations up to  $0.1^\circ$ . Since then various studies using the homemade SPR set-up have been done. A recent study, Nurrohman (2017) examined the growth of  $\text{Fe}_3\text{O}_4$  nanoparticles based microalgae using SPR resulting in  $26.2^\circ$  SPR angle shift. Oktivina (2017) reported the effect of  $\text{Fe}_3\text{O}_4$  nanoparticle concentration on the SPR signal. A concentration of 1 mg/ml shifts the SPR angle by  $0.1^\circ$ .

The SPR instrument that uses the scan angle of the resolution depends on how small the angle can be scanned (Schasfoort and McWhirter, 2008). Therefore, the smaller the angle that can be scanned the better the resolution. The resolution of the instrument is said to be high if it can distinguish SPR's angular change very clearly (Piliarik and Homola, 2006). Also, Luna-Moreno et al. (2015) categorize SPR instruments with angle scanning types having a high resolution when the resolution of the incident angle is 0.01 degrees.

The computerized system on SPR instruments has been done by Luna-Moreno et al. (2015) using LabView software as a virtual instrument that is user-friendly. The Labview device is used to control the rotation stage and data analyzer. Data analyzers can be used to compare theoretical predictions, simulations, and experimental results directly.

The SPR instrument employed by Luna-Moreno et al. (2015) uses a rotation stage to be able to vary prism angle variations automatically. The use of rotation stage itself has a deficiency that is the backlash. Backlash is a condition when the gear rotates and then rotates backwards with the same number of rounds, but the end position is not the same as the initial position. According to the rotation stage datasheet, it has a repeatability of five times its resolution. Therefore, it is essential to design a rotation stage that has a low backlash value or commonly called zero backlashes. According to Prodan et al., (2016) an instrument may be called a zero backlash when its repeatability approaches (or equals) its value of resolution.

One way to get the zero backlash is to design the gear in the rotation stage using a design gear that has been studied can reduce the backlash. Lindsay (2012) has designed a gear called Torsional Spring-Loaded Anti-backlash Gear, the design uses two gears on one axle but between the first and second gears have different pressure orientations. This design has been examined for performance before being encumbered by Yang et al. (2013) and its non-linear performance after being encumbered by Yang et al. (2015). Therefore, this design is appropriate for reducing the backlash so that the angle comes in the prism on the SPR instrument more accurately.

## 2. Research Methods

### 2.1. Mechanical Design

The design of the mechanical system consists of two-wheel gears, two worm gears, two stepper motors, place sensors, connecting axes, and retaining containers. The components are arranged in the illustrated Figure 1.

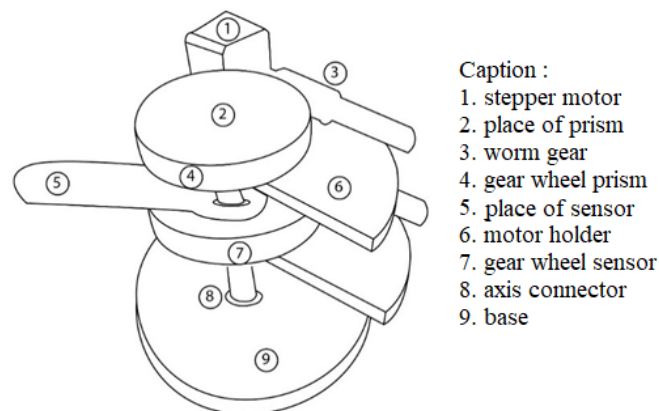


**Figure 1.** Design of the driving mechanics

Gir wheel has the advantage of high power efficiency, stable, accurate, and used in various mechanical systems. The main components of an anti-backlash gear are two-

wheeled gears and two springs coupled through the same axis. Figure 2 shows the Torsional Spring-Loaded Antibacklash gear model.

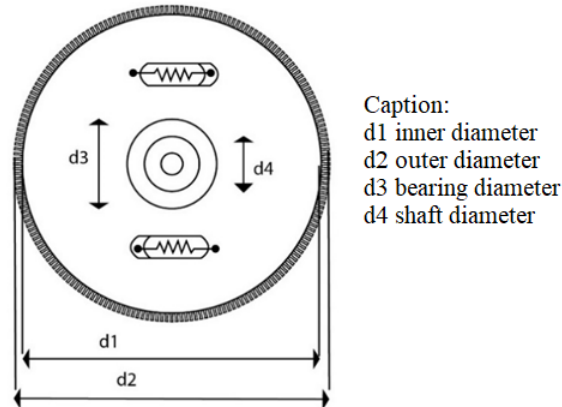


**Figure 2.** Sketch of front wheel gear design.

The shaft diameter between the sensor wheel gear, the prism wheel gear, and the stand is  $d_4$ . Between the first gear and the second gear can have a different direction of rotation, but there is a limit to how big the difference is because the spring limits it. When the first and second gears differ in the phase of the tooth the spring pulls them back into the same tooth phase. The recouping nature of the spring is used to reduce backlash.

The component of a mechanical system connected to the motor to drive the gear wheel is a worm gear. Gir worm is designed by calculating the density between the thread and its diameter. This worm gear is expected in one turn can only shift one gear wheel gear. The design of the worm gear is shown in Figure 3 with a threaded enclosure  $L_2$  and  $L_1$  diameter.

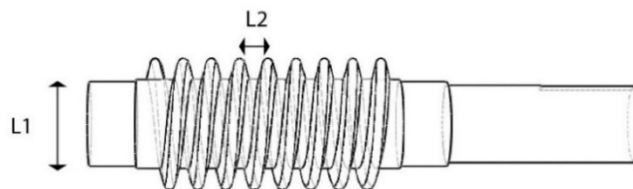


**Figure 3.** Sketch of the worm gear design.

## 2.2. Deposition of thin layer of gold

A thin layer of gold is obtained by evaporation using Jeep's JEE4X evacuator vacuum evaporator. The pressure in the chamber used is  $3 \times 10^{-3}$  Pa, the electric current is 50 A, and the distance of the boat to the closest prism is 11 cm. The prism is a semi-cylindrical prism. The gold mass that is varied is 17 mg for prisms A, B and C, 23 mg for D, E and F prisms and 25 mg for prisms G, H and I.

## 3. Result and Discussion

The driving mechanics of the homemade SPR set-up are shown in Figure 4. The ratio of the worm wheel gear is 1: 180 meaning 180 times the rotation of the worm gear is equal to one wheel rotation, so one round of worm gear only shifts the  $2^\circ$  gear wheel.

One step stepper motor rotates the shaft as much as  $1.8^\circ$  so to rotate  $360^\circ$  takes 200 steps. Therefore, a step stepper motor will rotate the gear wheel by  $0.01^\circ$ .

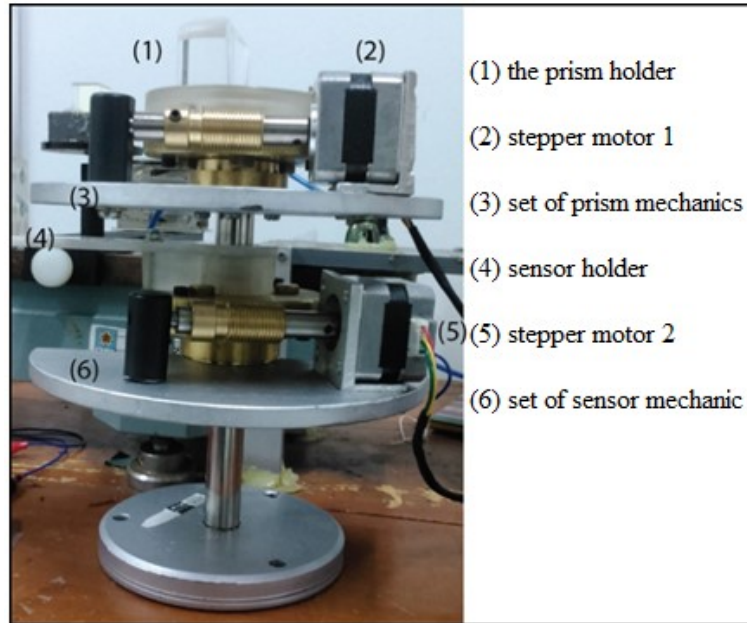


**Figure 4.** Mechanical system components.

System testing is performed on a computerized SPR set-up that was built by Laksono (2017). In the blank prism, the SPR curve is obtained as shown in Figure 5. The Total Internal Reflection (TIR) angle occurs at an angle of  $41.80^\circ$ . After the TIR angle, the reflectance is constant and no dip (decrease in intensity) due to the SPR phenomenon.

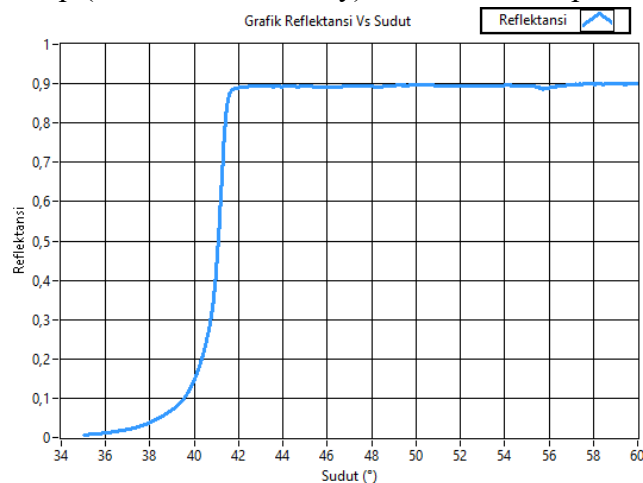


**Figure 5.** SPR curve on blank prism

Further testing is done on a prism that has been deposited a thin layer of gold. In a mass evaporation process of 17 mg, three prisms are at once placed in the chamber. Prisms A, B and C are placed on a horizontal holder 11 cm above the boat. The SPR curve obtained is shown in Figure 6. The SPR angle or resonance angle between the plasmon wave and the evanescent wave occurs at an angle of  $45.02^\circ$ ,  $45.05^\circ$ ,  $46.30^\circ$  for prisms A, B and C. Prism A and B are just above the boat, while the prism C has the furthest distance from the boat. Based on the simulation with the Winspall program, the

thickness of the gold thin film on prisms A, B and C is 28.9 nm, 28.5 nm, and 19.6 nm, respectively.

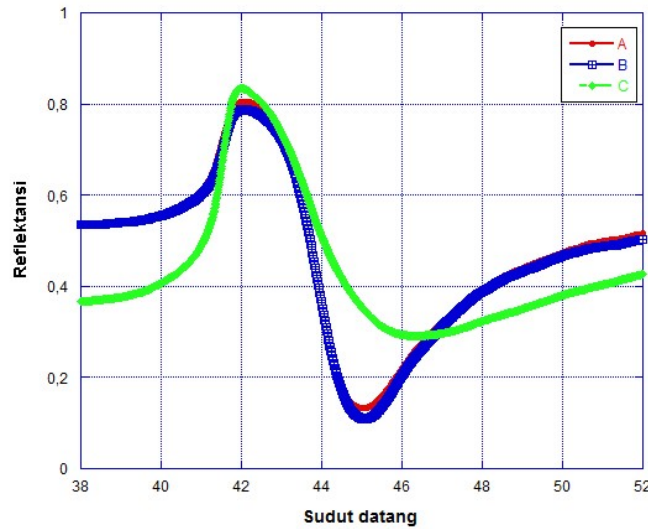


**Figure 6.** SPR curve on prism with evaporation mass of 17 mg.

The SPR curve of the D, E, F, G, H and I prisms is shown in Fig. 7. The obtained SPR angle is 44.48°, 44.70°, 45.49°, 45.52°, 45.66°, and 44.44°. This SPR angle correlates to the thickness of the thin film. The thinner the gold layer, the SPR angle will grow larger. The thickness of the obtained layer was 39.3 nm, 33.7 nm, 24.6 nm, 24.4 nm, 23.2 nm and 40.7 nm respectively.

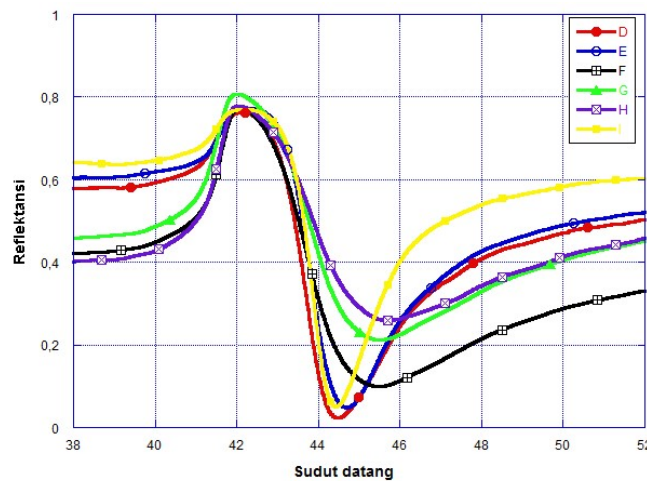


**Figure 7.** SPR curve on prism with evaporation mass 23 mg and 25 mg.

Based on the above results, it can be concluded that the effect of the thickness of the thin gold layer on the SPR angle shown in Figure 8. The prism distance to the boat determines the thickness of the resulting film. The thicker the gold layer obtained the smaller the SPR angle. In prism A and B, the difference of SPR angle of 0.03° shows the difference in thickness of the thin gold layer of 0.4 nm. It shows that a mechanical

system built with  $0.01^\circ$  prism rotation angle can detect a thin film thickness variation of 0.1 nm.

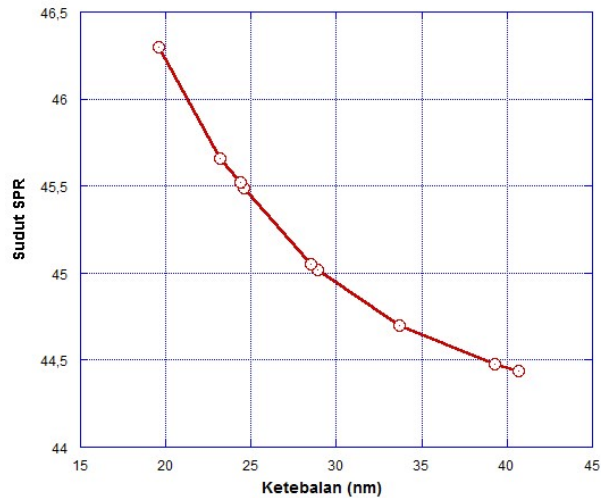


**Figure 8.** Effect of thick gold coating thickness on SPR angle.

#### 4. Conclusion

An optimized mechanical drive system has been performed at the homemade SPR set-up which has a  $0.01^\circ$  preloading angle resolution. The Spring-Loaded Torsional Model Antibacklash gear is used to improve the mechanical accuracy of the movers. The results showed that the built mechanical system was able to detect variations in the thickness of the gold thin film in the order of nanometers.

#### Acknowledgements

The authors would like to thank the research grants through the Research Grant Lecturer of Faculty of Mathematics and Natural Sciences of Universitas Gadjah Mada Fiscal Year 2017 with contract number 0070/J01.1.28/PL.06.02/2017.

#### References

- Arifin, M. (2011). Study of Surface Plasmon Resonance (SPR) Phenomena on Conductive Metals / Polymer Systems as Gas Sensors. Thesis. Yogyakarta: Faculty of Mathematics and Natural Sciences, Universitas Gadjah Mada.
- Lindsay, D. (2012). Anti-backlash resistant gearing for a seat mechanism. United State, US 7,735,927 B2.
- Luna-Moreno, D., Espinosa Sánchez, Y. M., Ponce de León, Y. R., Noé Arias, E., dan Garnica Campos, G. (2015). Virtual instrumentation in LabVIEW for multiple optical characterizations on the same optomechanical system. *Optik - International Journal for Light and Electron Optics*, 126(19), 1923–1929.
- Nasbei, H. (2009). Design of an Optical Observation System Surface Plasmon Resonance (SPR), Thesis. Yogyakarta: Faculty of Mathematics and Natural Sciences, Universitas Gadjah Mada.

- Nurrohman, D.T., Oktivina, M., Suharyadi, E., Suyono, E.A. and Abraha, K. (2017). Monitoring Microalgae Population Growth by using Fe<sub>3</sub>O<sub>4</sub> Nanoparticles-based Surface Plasmon Resonance (SPR) Biosensor. IOP Conference Series: Materials Science and Engineering, 202, 012077. DOI:10.1088/1757-899X/202/1/012077
- Oktivina, M., Nurrohman, D.T., Zaman, R.A.N.Q., Suharyadi, E., and Abraha, K. (2017). Effect of Fe<sub>3</sub>O<sub>4</sub> Magnetic Nanoparticle Concentration on the Signal of Surface Plasmon Resonance (SPR) Spectroscopy. IOP Conference Series: Materials Science and Engineering, 202,012032. DOI:10.1088/1757-899X/202/1/012032,
- Piliarik, M., dan Homola, J. (2006): SPR Sensor Instrumentation. Engineering, 4, 95–116, Berlin Heidelberg: Springer-Verlag.
- Prodan, D., Constantin, G., dan Teanu, A. B. Ş (2016). Eliminating The Backlash of Circular Feed Drivers of CNC Vertical Lathes. Proceedings in Manufacturing Systems, 11, 27–35.
- Schasfoort, R. B. M., dan McWhirter, A. (2008). SPR Instrumentation, Handbook of Surface Plasmon Resonance, 35–80, Cambridge: Royal Society of Chemistry.
- Yang, Z., Shang, J., Luo, Z., Wang, X., and Yu, N. (2015). Nonlinear Dynamics Modeling and Analysis of Torsional Spring-Loaded Antibacklash Gear with Time-Varying Meshing Stiffness and Friction. Advances in Mechanical Engineering, 5, 203438–203438.
- Yang, Z., Shang, J., Yu, N., Luo, Z., and Wang, X. (2013). Effects of shrink range and preload on dynamics characteristics of anti-backlash geared rotor-bearing system with composite mesh stiffness. Journal of Vibroengineering, 15(4), 1642.